Supplemental Information

Synthesis of OMC Powders:

The ordered mesoporous carbon denoted FDU-16 was synthesized by evaporation-induced organic-organic self assembly as previously reported [1]. Triblock copolymer F127 was dissolved in ethanol, then an ethanol solution of resol precursors phenol and formaldehyde was added and stirred for 10 minutes. The molar ratio of reagents used was phenol/formaldehyde/NaOH/F127 = 1:2:0.1:0.003-0.008. The homogenous mixture was poured into dishes and allowed to evaporate for 5-8 hours at room temperature, then placed in a 100° oven for 24 hours. The resulting film was scraped from the dish and ground into fine powder, then calcined in a tubular furnace under N_2 flow. The sample was heated to 600° C at the rate of 1° C/min, then to 900° C at the rate of 5° C/min, and held for two hours at 900° C.

The ordered mesoporous carbon denoted C-CS was synthesized from a carbon-silica nanocomposite produced by the evaporation-induced triconstituent co-assembly method [2]. Briefly, the triblock copolymer F127 was dissolved in ethanol with 0.2 M HCl and stirred for one hour at 40° C. Tetraethyl orthosilicate (TEOS) and 20% resol ethanolic solution were added, and stirring at 40° C continued for two hours. The initial mixture composition was F127/resol/TEOS/EtOH/HCl/H_2O = 1 : 0.5 : 2.08 : 12 : 7.3 x 10^{-3} : 1 in mass ratio. The mixture was then transferred to a dish, and the ethanol was evaporated at room temperature (5-8 hours) before thermopolymerization at 100° C for 24 hours. The resulting film was scraped from the dish and ground into fine powder, then calcined in a tubular furnace under N_2 flow. The sample was heated to 600° C at the rate of 1° C/min, then to 900° C at the rate of 5° C/min, and held for two hours at 900° C. The nanocomposite was immersed in 10% HF solution for 24 hours, which removed all of the silica to yield the 2-D hexagonal ordered mesoporous carbon C-CS. The C-CS, was rinsed thoroughly, then later put in dialysis tubing and rocked gently with Milli-Q water that was changed at least twice daily until constant conductivity of the water was measured. After dialysis, the C-CS powder was dried in an oven at 130° C.

A portion of both the FDU-16 and the C-CS mesoporous carbons were oxidized with acidic ammonia persulfate (APS, $(NH_4)_2S_2O_8$) according to the reported procedure [3], and will be called FDU-16-COOH, and C-CS-COOH, respectively. The carbon was added to 1.0 M APS solution, prepared in 2 M H_2SO_4, in the ratio of 1 g carbon per 60 mL APS solution. The mixture was stirred and refluxed in an air-proof round-bottom flask at 60° C for 12 hours. The OMCs were filtered, washed thoroughly with water and ethanol, then dried under vacuum overnight at 60° C.

Powder Addition method for PZC:

Sets of carbonate-free 0.1 M $NaClO_4$ solutions in polypropylene tubes, under argon, were adjusted to pH 3-10 with NaOH and $HClO_4$. The initial pH ($pH_{initial}$) values were measured with a pH electrode (Thermo Scientific Orion 8103BNUWP) before the carbon powders were added (1 g/L) and the tubes backfilled with argon. The samples were rocked gently for 24 hours,

and then the final pH (pH_{final}) was measured. Plots of ΔpH (pH_{final} - $pH_{initial}$) vs. $pH_{initial}$ were linear within the initial pH range 4 to 10, and the x-intercept was taken as the PZC. The experiment was duplicated and average PZC values reported.

Phase Separation in batch experiments:

LSC measurements of plutonium solutions after contact with the OMCs were taken after the solids were allowed to settle for at least 20 minutes. In Pu samples of C-CS-COOH, as well as all Pu batch kinetic experiments, a small aliquot was placed into a 0.5 mL capacity 30,000 MWCO regenerated cellulose centrifugal filter (Vivacon 500 series from Sartorius Stedim). Aliquots of 40 µL were centrifuged 12-15 minutes at 7000 rpm, and duplicate 10 µL aliquots of the filtrate were pipetted into LSC vials containing 5.0 mL of Ecolume scintillation cocktail. Control experiments with no solid sorbent showed no significant difference in Pu concentration between filtered aliquots and those taken directly. The percent sorption was calculated using equation S1, where C_i and C_f are the initial and final Pu concentrations, respectively. For samples from which more than one aliquot was removed, such as batch kinetic experiments, the value of C_i was corrected for solution volume and plutonium removed from previous assays.

$$\%sorption = \frac{C_i - C_f}{C_i} * 100\% \qquad \text{(S1)}$$

Phase separation in batch samples of OMCs with Eu solutions was achieved by centrifuging the samples for 2 minutes at 7000 rpm before duplicate 100 µL aliquots were pipetted into small conical vials for analysis by gamma counting. For timed batch experiments, the assay time was recorded at the beginning of centrifugation.

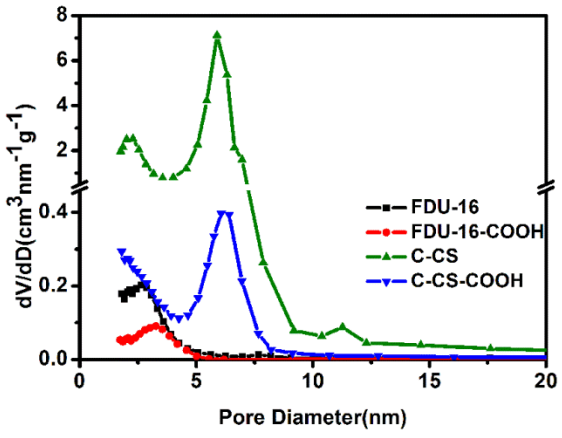

Figure S1. Pore size distributions of pristine and oxidized mesoporous carbons derived from N_2 adsorption data. The pore diameters in the primary mesopore networks of both FDU-16 and C-CS are slightly increased after wet oxidation.

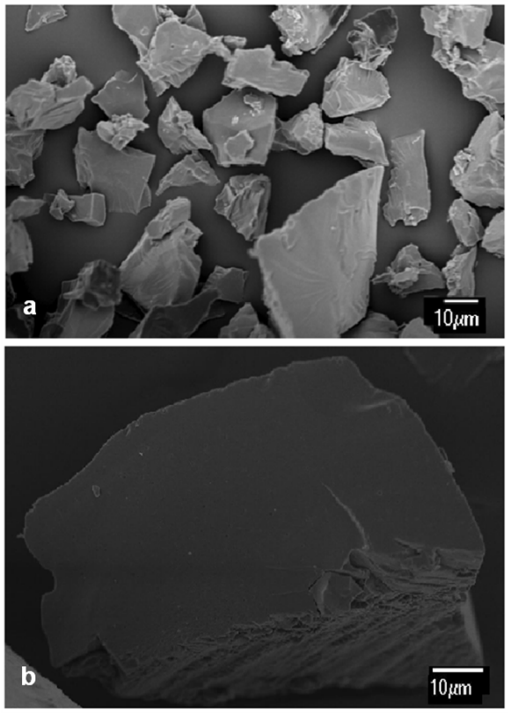

Figure S2: SEM images of C-CS (a) and FDU-16 (b) particles. No difference in particle size or morphology was observed after wet oxidation.

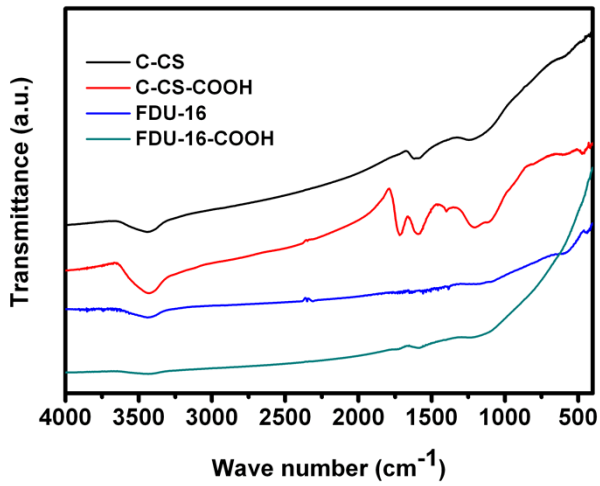

Figure S3: FTIR spectra of C-CS, C-CS-COOH, FDU-16, and FDU-16-COOH OMC powders

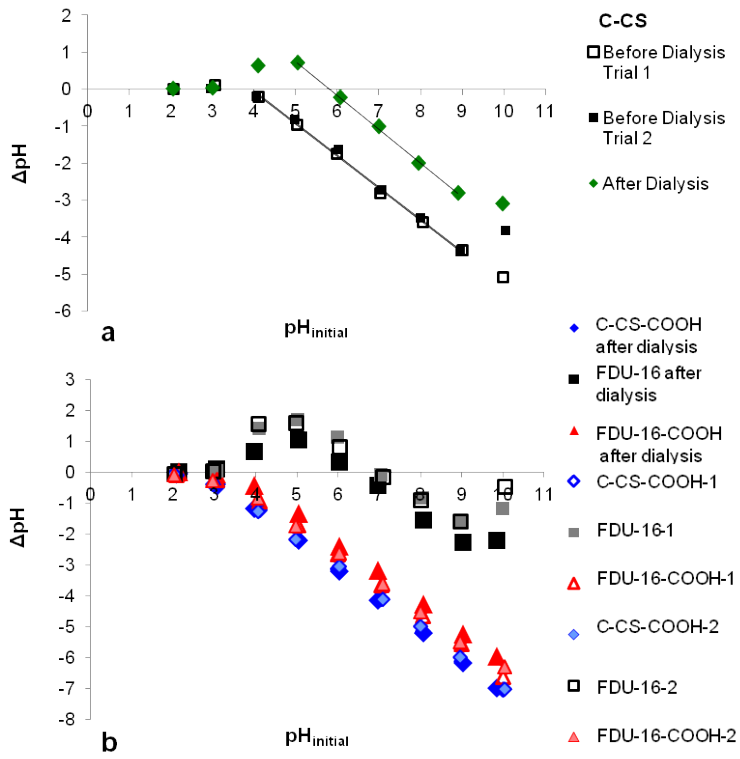

Figure S4. Plots of change in pH vs. initial pH from powder addition experiments with C-CS (a) and C-CS-COOH, FDU-16, FDU-16-COOH (b) before and after dialysis of the OMC powders. The C-CS powder underwent dialysis before being used for experiments with Pu and Eu, because the first measured PZC was lower than expected. The PZC after dialysis was considerably higher, perhaps due to the removal of trace HF and/or silica left from the synthesis. Dialysis of the other three OMC powders did not significantly alter their PZCs.

Batch kinetic data fits:

The batch kinetic data from the 10 µM samples were fit to pseudo-first-order, pseudo-second-order, and intra-particle diffusion model equations [4, 5], and a good fit (Figure S4) could only be achieved by the pseudo-second-order rate model, given in its linear form by equation S2:

$$\frac{t}{q_t} = \frac{1}{k_2 q_e^2} + \frac{t}{q_e} \qquad \text{(S2)}$$

where q_e is mg/g sorbed at equilibrium, q_t is mg/g sorbed at time t, k_2 is the second-order rate constant, and the term $k_2 q_e^2$ describes the initial sorption rate as t approaches 0. The satisfactory fit to this model suggests that the sorption mechanism is second order with respect to the carbon, and allows quantitative comparison between samples with the same experimental conditions. Table S1 summarizes the derived constants for the data presented in Figures 5 (a and c).

Table S1: Pseudo-second-order kinetic constants for batch C-CS and C-CS-COOH samples with pH 4 0.1 M $NaClO_4$ 10 ± 1 µM Pu(VI) solution.

Sample	$k_2 q_e^2$ (mg g^{-1}min^{-1})	k_2 (g mg^{-1}min^{-1})	q_e (mg/g)	R^2
C-CS 10 µM Eu	0.0230 ± 0.0002	0.051 ± 0.006	0.68± 0.04	0.9973
C-CS-COOH 10 µM Eu	10.8 ± 4.9	4.7 ± 2.0	1.526 ± 0.001	1
C-CS 10 µM Pu	0.11 ± 0.04	0.017 ± 0.004	2.5 ± 0.1	.9981
C-CS-COOH 10 µM Pu	13.6 ± 2.5	2.4 ± 0.4	2.40 ± 0.01	1

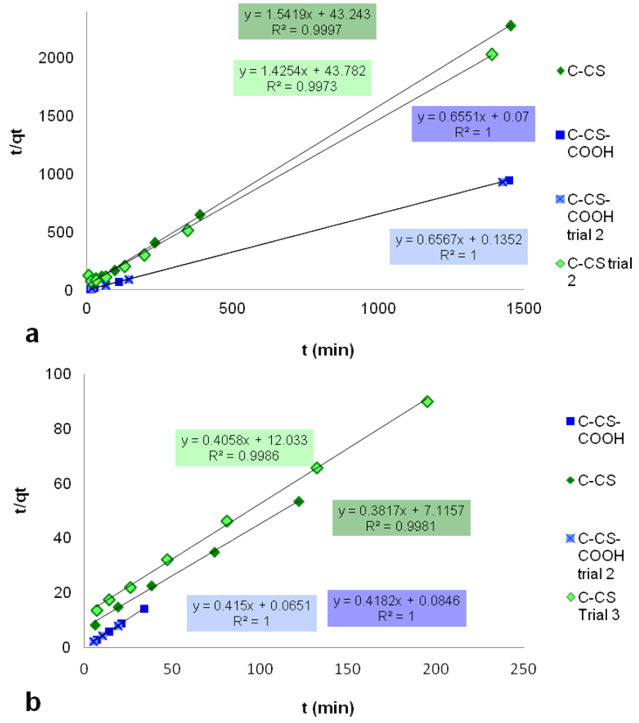

Figure S5. Pseudo-second-order kinetic model plots of data from batch C-CS samples with approximately 1000 mL/g of pH 4 0.1 M NaCl 10 ± 1 µM Eu solution (a) and pH 4 0.1 M $NaClO_4$ 10 ± 1 µM Pu solution (b).

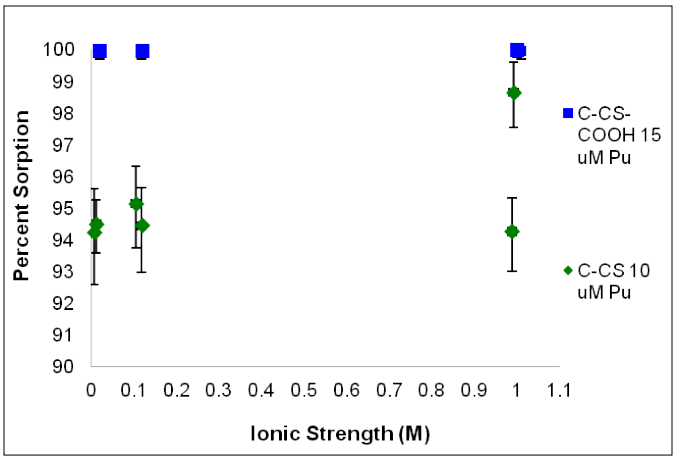

Figure S6. Percent Pu sorption vs. ionic strength for 10 µM Pu C-CS samples, and 15 µM Pu C-CS-COOH samples in pH 4 $NaClO_4$ solutions. Error bars represent 2σ.

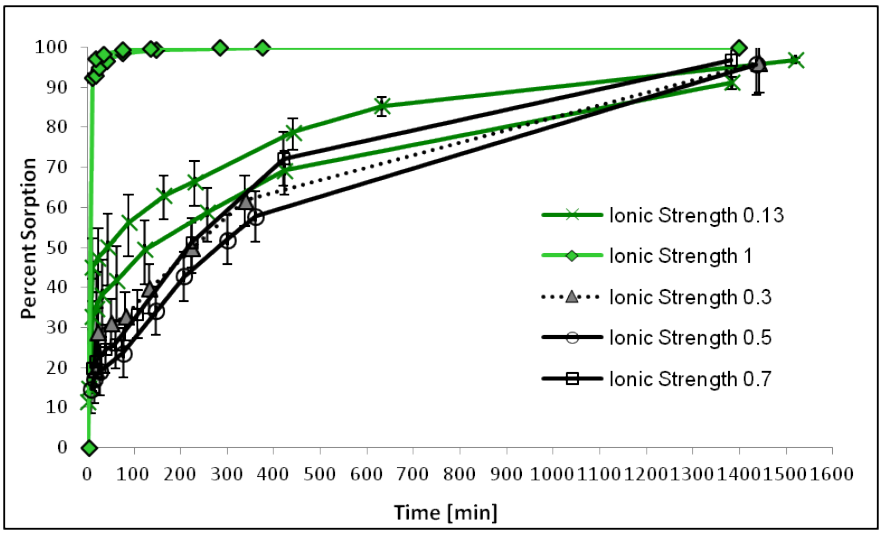

Figure S7. Percent sorption vs. minutes contact for C-CS carbon powder with 250 µM Pu, pH 4 $NaClO_4$ solutions of different ionic strengths. Lines are added to guide the eye; error bars represent 2σ.

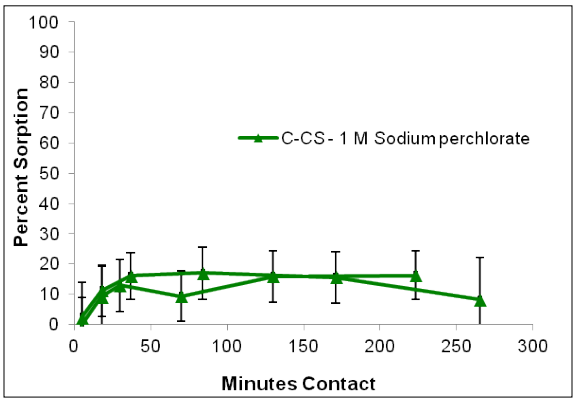

Figure S8. Percent sorption vs. minutes contact for batch C-CS samples with approximately 1000 mL/g of pH 4 1 M $NaClO_4$ 250 ± 15 µM Eu(III) solution. Lines are added to guide the eye; error bars represent 2σ.

Eu sortion isotherm fits:

The isotherm data were fit (Figure S8) to two common isotherm sorption models, Langmuir and Freundlich. The Langmuir model is given by equation 2, and assumes homogenous sorption of the target species in a monolayer fashion at specific binding sites in the sorbent.[6]

$$\frac{C_e}{q_e} = \frac{1}{bq_m} + \frac{C_e}{q_m} \quad \text{(S3)}$$

In equation S3 above, C_e is the equilibrium concentration of Eu in solution (µmol/mL), q_e is the corresponding amount of Eu bound to the solid (µmol/g), q_m is the monolayer sorption capacity (µmol/g), and b (mL/µmol) is the Langmuir adsorption constant related to the energy of adsorption. The Freundlich isotherm model is given by equation S4, and assumes a heterogeneous surface with a non-uniform distribution of heat-of-adsorption over the surface.[6]

$$\ln q_e = \ln K_F + \frac{1}{n} \ln C_e \quad \text{(S4)}$$

In equation S4 above, C_e and q_e have the same significance as in equation S3, and K_F and n are Freundlich constants related to the uptake capacity and energy of adsorption, respectively. In this model, values of n between 1 and 10 indicate a favorable sorption process. The Eu sorption isotherm for C-CS-COOH was best described by the Langmuir model, with a monolayer sorption capacity of 0.91 mmol/g (138 mg/g). The data from the C-CS isotherm did not fit well to either of these models, as the material showed low overall affinity for Eu. The parameters derived from fitting the isotherm data to these models are given in Table S2.

Table S2: Parameters derived from fitting C-CS and C-CS-COOH Eu sorption isotherms to Langmuir and Freundlich sorption models.

	Langmuir			**Freundlich**		
Sample	**q_m (µmol/g)**	**b (mL/µmol)**	**R^2**	**K_F (mL/µmol)**	**n**	**R^2**
C-CS-COOH	909.09	550	0.9993	5686	1.946	0.9151
C-CS	96.15	2.889	0.298	66.55	2.29	0.7903
C-CS omitting 1 mM	28.74	49.707	0.931	41.5	3.117	0.9071

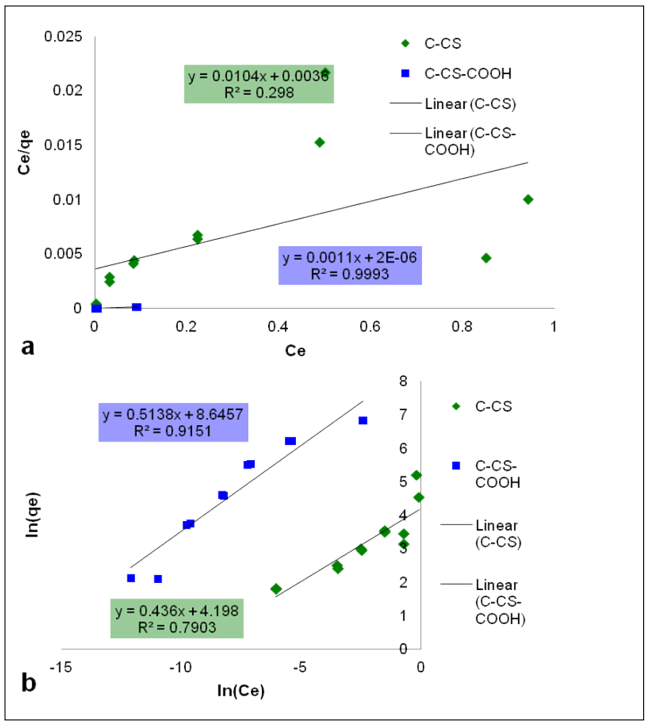

Figure S9. Langmuir (a) and Freundlich (b) sorption isotherm model plots of data from C-CS samples with approximately 1000 mL/g of pH 4 0.1 M NaCl solutions with Eu concentrations ranging from 10 µM to 1 mM.

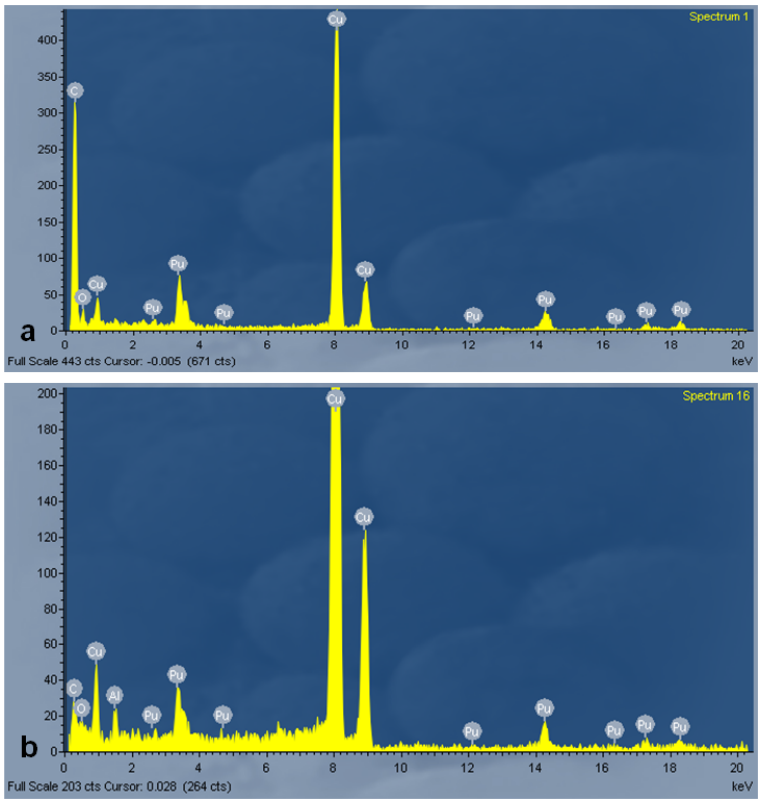

Figure S10. (a) Example X-ray EDS spectrum collected on C-CS particle shown in figure 8. Only Pu, O, and C were detected. (b) Example X-ray EDS spectrum collected on C-CS-COOH particle shown in figure 9 c and d. Al was detected along with Pu, O, and C. The Cu signal comes from the Cu TEM grid. The Cu signals in all EDS spectra come from the Cu TEM grid.

The bulk C-CS-COOH powder underwent dialysis following the TEM experiment, to remove any trace contaminants. Although some ions were excreted, the PZC measured by powder addition was the same before and after dialysis (see figure S2). The batch sorption of Pu from a pH 4, 0.1 M $NaClO_4$ 250 µM Pu(VI) solution was tested again, and the results after dialysis were the same as those from before (Figure S11). Therefore it seems unlikely that the trace elements present in TEM samples interfered with the interactions between Pu and C-CS-COOH.

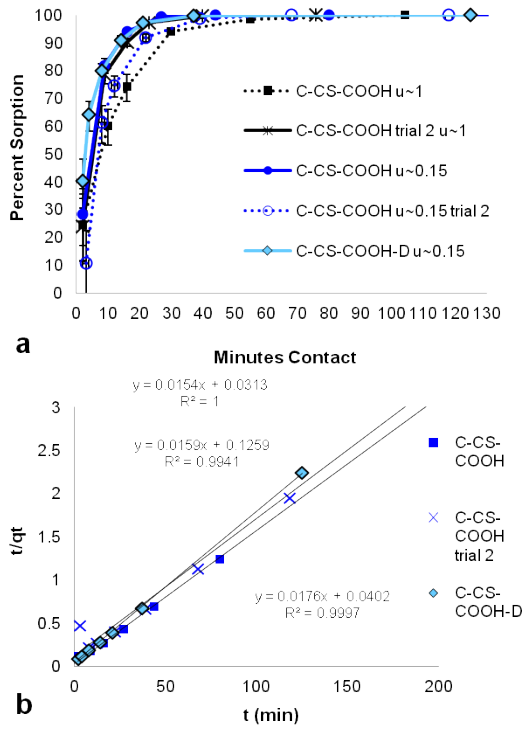

Figure S11. Percent Pu Sorption vs. minutes contact (a) and pseudo-second-order kinetic model plot (b)for batch C-CS-COOH samples with 250 ± 15 µM Pu(VI), 0.1 M $NaClO_4$, pH 4.0 ± 0.1 (except 1st and 2nd data points, which were always lower pH) . Lines in (a) are only to guide the eye, error bars represent 2σ. C-CS-COOH-D is the material after dialysis, and shows similar sorption behavior to the samples before dialysis.

XAS experimental details:

Pu L_{III} XAS spectra were collected on SSRL beamline 11-2 using a 30% detuned Si(220) φ-0° double-crystal monochromator. The carbon sample spectra were collected at 30 ± 2 K, using a specially engineered liquid helium cryostat (Janis) to mitigate beam-induced reduction of Pu in the samples. Data were collected in fluorescence mode using a 100-element germanium detector. The vertical aperture of the beam was adjusted between approximately 0.25 mm to 0.50 mm to avoid overloading the detector. Energy calibration was performed by measuring the inflection point in the plutonium L_{III}-edge of a $^{242}PuO_2$ powder, 18062.3 eV,[7] in transmission mode between samples, at room temperature. At least 10 scans per sample were acquired, using 1 second per point in the pre-edge and edge regions, increasing to 8 seconds per point at k = 14. The fluorescence spectra were dead time corrected using the method of Webb.[8]

Linear combination analysis (LCA) fitting of the X-ray absorption near edge structure (XANES) spectra was accomplished using the program ATHENA. Extended X-ray absorption fine structure (EXAFS) analysis utilized the programs ATHENA and ARTEMIS [9] for data reduction and modeling, respectively. To determine the amount of PuO_2 present in the samples, as opposed to Pu(IV) sorbed to the surface with no long range Pu-Pu order, the EXAFS data were fit using paths generated by FEFF6.[10-13] Fitting of the PuO_2 standard used the first and second shell oxygen and plutonium single scattering paths, and eight associated

multiple scattering paths. Using variables from the single scattering paths to account for changes in the multiple scattering paths minimized the number of fitting variables used. In the end, a total of 7 variables were used for the entire fit consisting of 11 paths. An 8th variable was added, representing the contribution of PuO_2 to the sample's spectrum, which was fit simultaneously with the PuO_2 standard. The number of independent points using the adjusted Nyquist formula[14] was 38.

1. Y. Meng, D. Gu, F. Q. Zhang, Y. F. Shi, L. Cheng, D. Feng, Z. X. Wu, Z. X. Chen, Y. Wan, A. Stein and D. Y. Zhao, *Chemistry of Materials*, 2006, **18**, 4447-4464.
2. R. L. Liu, Y. F. Shi, Y. Wan, Y. Meng, F. Q. Zhang, D. Gu, Z. X. Chen, B. Tu and D. Y. Zhao, *Journal of the American Chemical Society*, 2006, **128**, 11652-11662.
3. Z. Wu, P. A. Webley and D. Zhao, *Langmuir*, 2010, **26**, 10277-10286.
4. G. Tian, J. Geng, Y. Jin, C. Wang, S. Li, Z. Chen, H. Wang, Y. Zhao and S. Li, *Journal of Hazardous Materials*, 2011, **190**, 442-450.
5. L. Y. Yuan, Y. L. Liu, W. Q. Shi, Y. L. Lv, J. H. Lan, Y. L. Zhao and Z. F. Chai, *Dalton Transactions*, 2011, **40**, 7446-7453.
6. H. M. H. Gad and N. S. Awwad, *Separation Science and Technology*, 2007, **42**, 3657-3680.
7. S. D. Conradson, K. D. Abney, B. D. Begg, E. D. Brady, D. L. Clark, C. den Auwer, M. Ding, P. K. Dorhout, F. J. Espinosa-Faller, P. L. Gordon, R. G. Haire, N. J. Hess, R. F. Hess, D. W. Keogh, G. H. Lander, A. J. Lupinetti, L. A. Morales, M. P. Neu, P. D. Palmer, P. Paviet-Hartmann, S. D. Reilly, W. H. Runde, C. D. Tait, D. K. Veirs and F. Wastin, *Inorganic Chemistry*, 2003, **43**, 116-131.
8. S. M. Webb, *Physica Scripta*, 2005, **T115**, 1011-1014.
9. B. Ravel and M. Newville, *Journal of Synchrotron Radiation*, 2005, **12**, 537–541.
10. J. J. Rehr, J. M. Deleon, S. I. Zabinsky and R. C. Albers, *Journal of the American Chemical Society*, 1991, **113**, 5135-5140.
11. J. J. Rehr, R. C. Albers and S. I. Zabinsky, *Physical Review Letters*, 1992, **69**, 3397-3400.
12. J. J. Rehr and R. C. Albers, *Physical Review B*, 1990, **41**, 8139-8149.
13. J. M. Deleon, J. J. Rehr, S. I. Zabinsky and R. C. Albers, *Physical Review B*, 1991, **44**, 4146-4156.
14. E. A. Stern, *Physical Review B*, 1993, **48**, 9825-9827.